Principal optical constants measurement of uniaxial crystal CdSe in the wavelength region between 380 and 950 nm

M. Schäffner, X. Bao, and A. Penzkofer

The principal optical constants n_o, κ_o, n_e, and κ_e of the hexagonal crystal CdSe are determined in the wavelength region between 380 and 950 nm at room temperature. The minimum reflectivities and the corresponding Brewster angles of parallel polarized light are measured for ordinary and extraordinary rays in the wavelength region between 380 and 728 nm. At longer wavelengths ($\kappa_o < 10^{-3}$) Brewster-angle measurements and transmission measurements were applied. A plot of the absorption coefficients α_o and α_e versus wavelength indicates deviations from a direct band-gap parabolic absorption dependence.
Key words: Optical constants, refractive-index measurement, absorption coefficient measurement, CdSe, optical constants of uniaxial crystals.

1. Introduction

The hexagonal CdSe crystal is a direct-gap II–VI semiconductor of $P6_3mc$ (C_{6v}^4) space group and 6mm (C_{6v}) point group symmetry (wurtzite lattice structure).[1,2] The optical indicatrix is uniaxial. Its energy gap is $E_g(0\ \mathrm{K}) = 1.841\ \mathrm{eV} = 14\,838\ \mathrm{cm}^{-1} = 674$ nm at zero temperature and $E_g(293\ \mathrm{K}) = 1.751\ \mathrm{eV} = 14\,112\ \mathrm{cm}^{-1} = 708.6$ nm at room temperature.[2,3]

In the transparent near-IR spectral region, below the energy gap, the dispersion of the principal ordinary n_o and the extraordinary index of refraction n_e is well known.[2,4–10] The optical birefringence, $\Delta n = n_e - n_o$, was determined with high accuracy mainly by interference measurements between crossed polarizers.[5,7–9,11–14] The absorption behavior in the subgap-frequency region depends on the impurity content and on the charge compensation.[6,15–17] Detailed absorption measurements at the band edge are reported in Refs. 11, 12, 15, 16, 18, and 19.

There is little information about the optical constants of CdSe above the energy gap.[20] The principal refractive indices (n_o, n_e) and the principal extinction coefficients (κ_o, κ_e) of CdSe have been determined over a wide energy range from 0 to 10 eV by reflection measurement and the Kramers–Kronig analysis.[20] The determined dispersion of the optical constants confirmed the band-structure scheme of CdSe.[20–22] In thin CdSe films the anisotropy-averaged optical constants $\bar{n}$ and $\bar{\kappa}$ have been measured in the visible and the near-IR spectral region.[23–25] The data were determined by transmission and reflection measurements. Band-gap data were extracted from the wavelength dependence of the extinction coefficient.[25]

We determine the principal optical constants $n_o(\lambda)$, $\kappa_o(\lambda)$, $n_e(\lambda)$, and $\kappa_e(\lambda)$ of a Se-treated compensated CdSe hexagonal single crystal (from Cleveland Crystals Company) at room temperature. The wavelength region that we analyzed is between 380 and 950 nm. For $\lambda < 728$ nm the absorption is high and the optical constants are determined from the minimum reflectivity of parallel polarized light $R_{\parallel,\min}$ and the corresponding angle of incidence ϕ_B (the generalized Brewster angle). The measurement technique was applied previously to isotropic strongly absorbing media.[26] Here the method is extended to the determination of the principal optical constants of optical uniaxial crystals. In our measurements on CdSe an accuracy of $\Delta n/n \approx \pm 0.003$ and $\Delta\kappa/\kappa \approx \pm 0.03$ was achieved. For $\lambda > 728$ nm the transmission becomes measurable and the optical constants are determined from normal-incidence transmission and Brewster-angle measurements. Above 800 nm our refractive-index results are compared with the published data obtained by refractive measurements.[4,5]

The measured absorption spectra are discussed in terms of the band-structure scheme of CdSe. A detailed knowledge of the dispersion of the refractive indices is necessary for phase-dependent nonlinear optical processes such as second-harmonic generation. The refractive-index data of CdSe were needed in an analysis of the competition between resonant second-harmonic generation and two-photon absorption in

When this work was done all authors were with the Naturwissenschaftliche Fakultät II–Physik, Universität Regensburg, W-8400 Regensburg, Germany. X. Bao is now with the Department of Physics and Applied Physics, University of Strathclyde, Glasgow, Scotland.

Received 6 August 1991.
0003-6935/92/224546-07$05.00/0.

CdSe where the resonant second-harmonic susceptibilities were determined.[27]

2. Experiment

The experimental arrangement for the oblique reflection measurements is sketched in Fig. 1(a). Details of the setup are reported in Ref. 26. A tungsten lamp is used as a light source. The light is polarized parallel to the plane of incidence with a Glan polarizer. The angle of incidence ϕ to the CdSe sample S is varied with the rotation stage R1. The rotation stage R2 directs the reflected light to the spectrometer SP. The spectral distribution of the reflected light is recorded with a diode array system (Tracor type DARSS). For calibration reference spectra are measured with a glass prism totally reflecting the incident light. The crystal size is $1 \times 12 \times 12$ mm^3. Its optical axis c is parallel to a 12-mm edge. The minimum reflection $R_{\parallel,\min}$ and its angle of incidence ϕ_B (the generalized Brewster angle) of parallel polarized light are determined and applied to the calculation of the optical constants.

The crystal orientations are indicated in Figs. 1(b) and 1(c). The ordinary principal constants n_o and κ_o are determined with the arrangement in Fig. 1(b). (The optic axis c is perpendicular to the plane of incidence.) The extraordinary optical constants $n_{ao}(\phi_B)$ and $\kappa_{ao}(\phi_B)$ are determined with the arrangement in Fig. 1(c). (The c axis is parallel to the crystal surface in the plane of incidence.) The principal extraordinary constants n_e and κ_e are calculated from the measured values of $n_{ao}(\phi_B)$, $\kappa_{ao}(\phi_B)$, n_o, and κ_o by applying the generalized Snell's law for absorbing media.[28–32]

For $\lambda > 728$ nm normal-incidence transmission measurements $[T(\lambda)]$ were carried out on a commercial spectrophotometer, and the Brewster angle $\phi_B(\lambda)$ was obtained by $R_{\parallel,\min}$ determination with the experimental arrangement in Fig. 1(a).

The reflection measurements probe the sample surface down to a thickness d_P determined either by the penetration depth α^{-1} or by the light wavelength in matter λ/n, i.e., $d_P \approx \min(\alpha^{-1}, \lambda/n)$. An adsorbed layer of $d_{ad} \ll \lambda$ thickness modifies the measured optical constants by a factor of $\sim 1 + (n_A - n_{ad})(n - n_{ad})d_{ad}/\lambda$, where $n_A \approx 1$ is the refractive index of air and n_{ad} is the refractive index of the absorbed layer (Chap. I.6 of Ref. 31). The modification is generally negligible. In our experiments we cleaned the crystal surfaces with isopropyl alcohol to exclude contributions from adsorption layers.

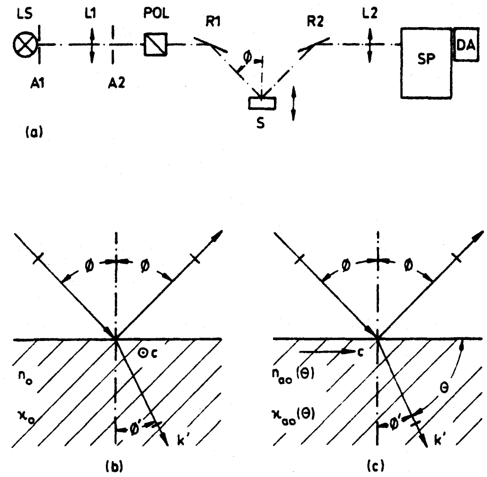

Fig. 1. (a) Schematic of experimental setup: LS, light source (tungsten lamp); L1, collimating optics; L2, lens, A1, A2, apertures; POL, Glan polarizer; R1, R2, aluminum mirrors on rotation stages; S, sample on the translation and tilting stage; SP, spectrometer; DA, diode array system. (b) Ordinary ray tracing. (c) Extraordinary ray tracing. $\mathbf{k}'$ is the wave vector in crystal.

The optical constants of the crystal surface itself may deviate from the bulk optical constants within a thickness $d_{ex} \approx 2a_{ex}$, where $a_{ex} = a_B\epsilon_r m/m_{ex}$ is the exciton Bohr radius.[33] For CdSe it is $a_{ex} \approx 5$ nm (electronic Bohr radius $a_B = 0.0529$ nm, static dielectric constant $\epsilon_r \approx 9.4$,[2] effectively reduced exciton mass ratio $m_{ex}/m \approx 0.1$,[2] where m is the mass of a free electron, $m_{ex}^{-1} = m_e^{-1} + m_h^{-1}$). In this sense we measure effective optical constants averaged over the thickness d_P. Their deviations from the bulk values are thought to be small because d_{ex} is still small compared with α^{-1} (≈ 90 nm at $\lambda = 500$ nm) or λ/n (≈ 190 nm at $\lambda = 500$ nm).

3. Theory

The extraction of the optical constants from the measurement of the minimum reflection of parallel polarized light $R_{\parallel,\min}$ at the generalized Brewster angle ϕ_B and from normal-incidence transmission T and Brewster angle ϕ_B measurements is considered in the following.

A. Minimum Reflection of Parallel Polarized Light

The light reflection is determined by the Fresnel laws.[28–32] For parallel polarized light incident at an angle ϕ to the crystal the reflectivity is[26,34]

$$R_\parallel = \left| \frac{\left(\dfrac{\tilde{n}}{n_A}\right)^2 \cos\phi - \cos\chi}{\left(\dfrac{\tilde{n}}{n_A}\right)^2 \cos\phi + \cos\chi} \right|^2 = \left| \frac{\left(\dfrac{\tilde{n}}{n_A}\right)^2 \cos\phi - \left(\dfrac{\tilde{n}^2}{n_A{}^2} - \sin^2\phi\right)^{1/2}}{\left(\dfrac{\tilde{n}}{n_A}\right)^2 \cos\phi + \left(\dfrac{\tilde{n}^2}{n_A{}^2} - \sin^2\phi\right)^{1/2}} \right|^2$$

$$= \frac{(C^2 + D^2)\cos^2\phi + A - 2A^{1/2}\cos\phi(C\cos B + D\sin B)}{(C^2 + D^2)\cos^2\phi + A + 2A^{1/2}\cos\phi(C\cos B + D\sin B)}, \tag{1}$$

where $A = [(n^2/n_A^2 - \kappa^2/n_A^2 - \sin^2\phi)^2 + 4n^2\kappa^2/n_A^4]^{1/2}$, $B = 0.5 \times \arctan\{2n\kappa/[n_A^2(n^2/n_A^2 - \kappa^2/n_A^2 - \sin^2\phi)]\}$, $C = (n^2 - \kappa^2)/n_A^2$, and $D = 2n\kappa/n_A^2$, $\tilde{n} = n - i\kappa$ is the complex refractive index of the crystal, and n_A is the refractive index of air. A dispersion formula for $n_A(\lambda)$ is given in Ref. 35; $n_A = 1$ is used in our calculations. The second equality of Eq. (1) is obtained by use of the generalized Snell's law $\sin\phi = (\tilde{n}/n_A)\sin\chi$, where χ is the complex refraction angle.

The values n and κ are determined from the minimum reflectivity $R_{\parallel,\min}$ at the generalized Brewster angle ϕ_B. For the c axis that is perpendicular to the plane of incidence [Fig. 1(b)], $R_{\parallel,\min}(\phi_B)$ gives the ordinary refractive index n_o and the ordinary extinction coefficient κ_o. For the c axis that is parallel to the plane of incidence [Fig. 1(c)], $R_{\parallel,\min}(\phi_B)$ gives the extraordinary constants n_{ao} and κ_{ao}, which depend on the angle ϕ_B. For the determination of the principal extraordinary optical constants n_e and κ_e, the angle $\theta_B = \pi/2 - \phi_B'$ between the optic axis c and the constant-phase propagation direction k' in the crystal has to be known [Fig. 1(c)], ϕ_B' is related to ϕ_B by Snell's law[31,32]:

$$\phi_B' = \arcsin\left(\frac{n_A \sin\phi_B}{n_T}\right), \tag{2}$$

with

$$n_T = (n_A^2 \sin^2\phi_B + \eta^2\cos^2\beta)^{1/2}, \tag{3}$$

where η and β are implicitly given by

$$\eta^2\cos(2\beta) = n_{ao}^2 - \kappa_{ao}^2 - n_A^2\sin^2\phi_B, \tag{4}$$

$$\eta^2 \sin 2\beta = 2n_{ao}\kappa_{ao}. \tag{5}$$

Explicit equations for β and η are obtained from Eqs. (4) and (5). They read

$$\beta = 1/2 \arctan\left(\frac{2n_{ao}\kappa_{ao}}{n_{ao}^2 - \kappa_{ao}^2 - n_A^2\sin^2\phi_B^2}\right), \tag{6}$$

$$\eta = \left[\frac{2n_{ao}\kappa_{ao}}{\sin(2\beta)}\right]^{1/2}. \tag{7}$$

n_{ao} is related to n_o and n_e by

$$\frac{1}{n_{ao}^2} = \frac{\cos^2\theta_B}{n_o^2} + \frac{\sin^2\theta_B}{n_e^2}. \tag{8}$$

Solving Eq. (8) gives

$$n_e = \frac{\sin(\theta_B)}{\left[\dfrac{1}{n_{ao}^2} - \dfrac{\cos^2\theta_B}{n_o^2}\right]^{1/2}}. \tag{9}$$

The relationship between κ_{ao} and the principal optical constants is[31]

$$\frac{\kappa_{ao}}{n_{ao}^2} = \kappa_o\frac{\cos^2\theta_B}{n_o^2} + \kappa_e\frac{\sin^2\theta_B}{n_e^2}, \tag{10}$$

leading to

$$\kappa_e = \left(\frac{\kappa_{ao}}{n_{ao}^2} - \frac{\kappa_o\cos^2\theta_B}{n_o^2}\right)\frac{n_e^2}{\sin^2\theta_B}. \tag{11}$$

The absorption coefficient α is related to the extinction coefficient κ by

$$\alpha = 4\pi\tilde{\nu}\kappa = 4\pi\kappa/\lambda, \tag{12}$$

where $\tilde{\nu} = c_0/\nu = 1/\lambda$ is the wave number, where ν is the frequency, c_0 is the vacuum light velocity, and λ is the wavelength of light in vacuum.

B. Normal-Incidence Transmission and Brewster-Angle Measurement

In the case of small absorption ($\kappa \lesssim 10^{-3}$) the Brewster angle ϕ_B is determined solely by the refractive index n.[26] The minimum reflectance $R_{\parallel,\min}(\phi_B)$ of parallel polarized light becomes small, and its absolute measurement becomes inaccurate because of scattering contributions. Therefore κ is more precisely determined by normal-incidence transmission measurements.

The normal-incidence transmission through the sample is given by (p. 9 of Ref. 36)

$$T = \frac{(1-R)^2\exp(-\alpha l)(1+\kappa^2/n^2)}{1 - R^2\exp(-2\alpha l)}, \tag{13}$$

where the normal-incidence reflection R is

$$R = \frac{(n-1)^2 + \kappa^2}{(n+1)^2 + \kappa^2}. \tag{14}$$

The refractive indices are determined by the procedure described in Subsection 3.A (ϕ_B measurement), and κ is calculated from the transmission measurements by solving Eq. (13) numerically.

4. Results

The minimum parallel reflectivities $R_{\parallel,\min}$ of the ordinary and extraordinary rays versus wavelength λ are shown in Fig. 2. In the long-wavelength region $\lambda \gtrsim 730$ nm a background reflection of $R_\parallel \approx 4 \times 10^{-4}$ was obtained for both crystal arrangements. This background level is assumed to be independent of wavelength and is subtracted for the calculation of the optical constants. The normal-incidence transmissions T are included in Fig. 2. The generalized Brewster angles ϕ_B are displayed in Fig. 3.

The resulting dispersion of the principal refractive indices, n_o and n_e, is shown in Fig. 4. The wavelength dependence of the principal extinction coefficients, κ_o and κ_e, is displayed in Fig. 5. The absorption coefficients, α_o and α_e, are shown by the solid curves in Fig. 6.

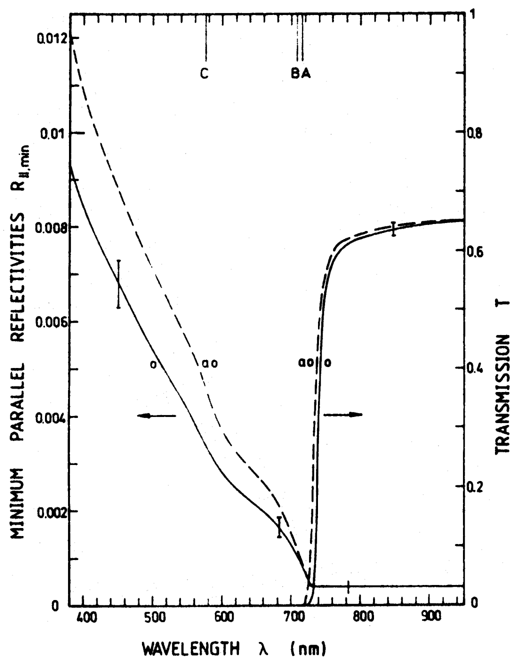

Fig. 2. Minimum parallel reflectivities $R_{\parallel,\mathrm{min}}$ at the generalized Brewster angle ϕ_B and transmissions T at normal incidence. The exciton transition edges A, B, and C are indicated.

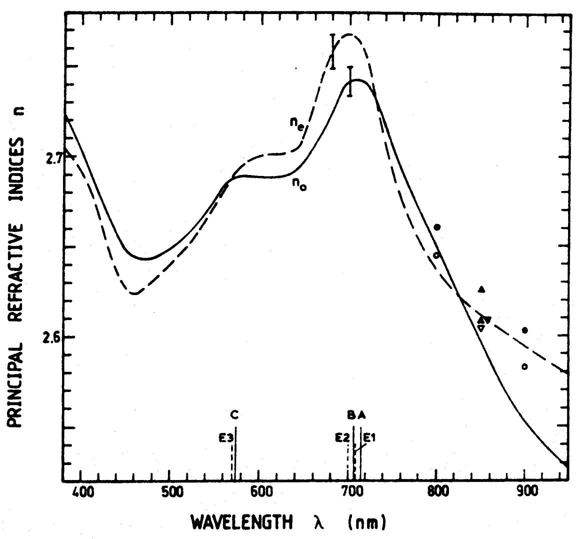

Fig. 4. Principal refractive indices n_o and n_e of CdSe versus wavelength. The points are taken from Ref. 4 (○, ●), Ref. 5 (△, ▲) and Ref. 9 (▽, ▼). The open symbols belong to n_o, and the filled symbols belong to n_e. The absorption band edges $E1$, $E2$, $E3$ and the exciton transition edges A, B, and C are indicated.

5. Discussion

The $\phi_B(\lambda)$ curves (Fig. 3) and $n(\lambda)$ curves (Fig. 4) have a similar structure indicating that n is mainly determined by ϕ_B and only slightly influenced by $R_{\parallel,\mathrm{min}}$.[26] The $R_{\parallel,\mathrm{min}}(\lambda)$ curves (Fig. 2) and $\kappa(\lambda)$ curves (Fig. 5) also have similar shapes revealing the dependence of $R_{\parallel,\mathrm{min}}$ on κ. In Fig. 4 some published refractive-index data in the transparent spectral region are included.[4,5,9] Our refractive indices agree within $\delta n = 0.03$ with the reported data.

In our measurements three isotropic wavelength points (inversion points) at $\lambda \approx 825$, 730, and 570 nm are observed where the refractive indices n_o and n_e are equal. A crossing or touching of the n_o and n_e curves around 410 nm cannot be excluded. An inversion point at $\lambda = 735$ nm (709.5 nm) was reported in Ref. 13 (14). The birefringence data, $n_e - n_o$, of Ref. 8 indicate an inversion point at 800 nm.

The reported thin-film studies did not distinguish between ordinary and extraordinary optical constants.[23–25] The average n and κ data agree qualitatively with our measurements. The optical constants determined by a Kramers–Kronig analysis over a wide energy range from 0 to 10 eV (Ref. 20) are

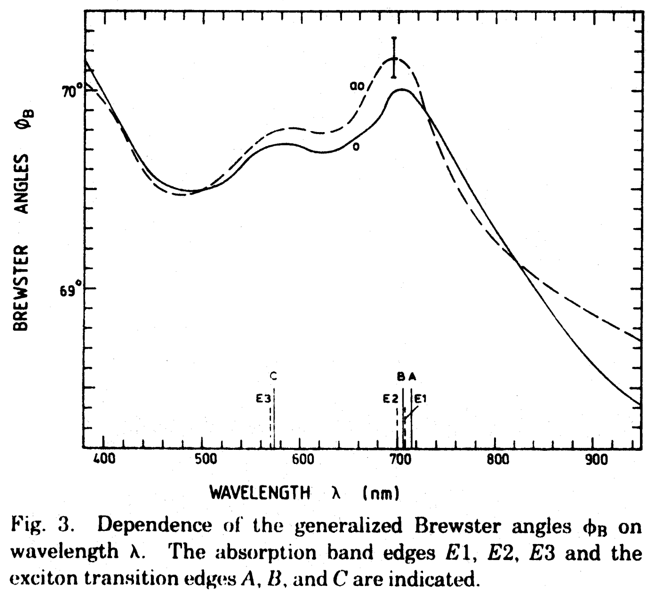

Fig. 3. Dependence of the generalized Brewster angles ϕ_B on wavelength λ. The absorption band edges $E1$, $E2$, $E3$ and the exciton transition edges A, B, and C are indicated.

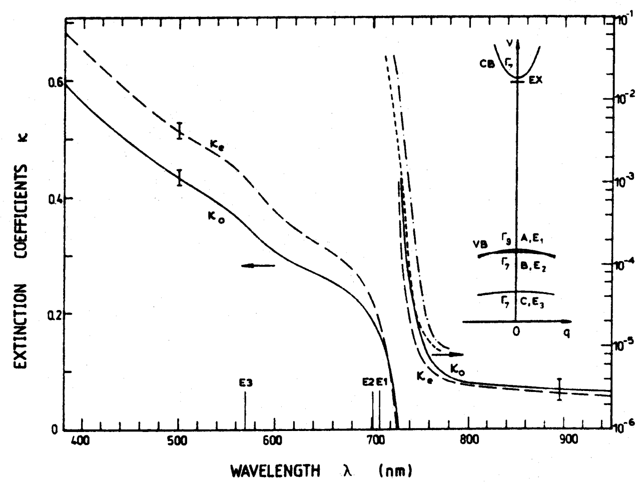

Fig. 5. Principal extinction coefficients κ_o and κ_e of CdSe versus wavelength. Band edges $E1$, $E2$, and $E3$ are indicated. Solid and long-dashed curves are our own measurements. The dashed–dotted curve κ_o and the short dashed curve κ_e are redrawn from Ref. 18. The inset shows part of the energy band structure of CdSe at Γ point (the center of the Brillouin zone): CB, the lowest lying conduction band; VB, the topmost-lying three valence bands; EX, the indication of exciton-binding energy; q, the Brillouin zone coordinate.

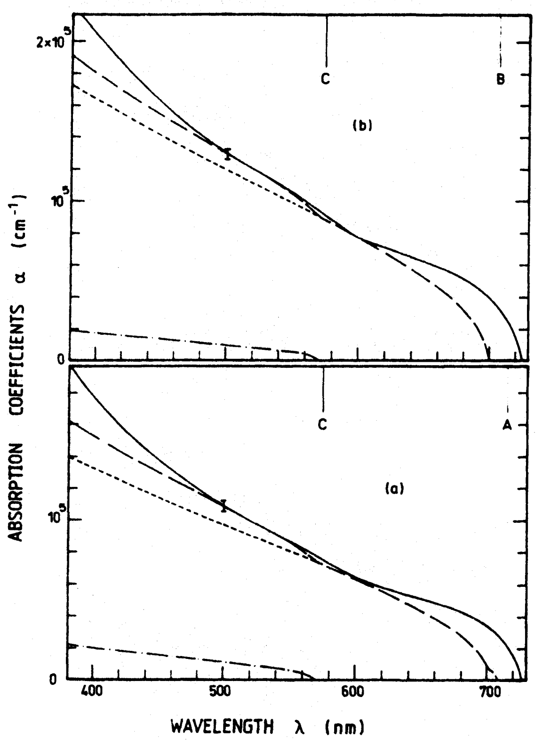

Fig. 6. Principal absorption coefficients α_o (a) and α_e (b) of CdSe. The solid curves are experimental results. The dashed curves are parabolic direct-gap theoretical fits [Eq. (15)] to the experimental data at 600 and 500 nm. The fit parameters are $\beta_{o,1}' = \beta_{o,2}' = 2.0126 \times 10^6\ \mathrm{cm^{-1}\,nm^{1/2}}$, $\beta_{o,3}' = 7.395 \times 10^5\ \mathrm{cm^{-1}\,nm^{1/2}}$, $\beta_{e,1}' = 0$, $\beta_{e,2}' = 4.977 \times 10^6\ \mathrm{cm^{-1}\,nm^{1/2}}$, and $\beta_{e,3}' = 6.303 \times 10^5\ \mathrm{cm^{-1}\,nm^{1/2}}$. The short-dashed curves show contributions of the $E1$ and $E2$ band transitions. The dashed–dotted curves indicate the contribution of the $E3$ band transition. The exciton band edges A, B, and C are indicated.

more crude than our data in the energy range from 1.3 to 3.25 eV. Some absorption coefficients above the energy gap were derived in Ref. 37 from photoluminescence measurements in an electrochemical cell by application of a dead-layer model.

Part of the band structure of CdSe around the Γ point is included in Fig. 5.[2] The transition from the topmost light-hole valence band to the conduction band is $E1$, the transition from the crystal-field, split-off, heavy-hole valence band to the conduction band is $E2$, and the transition from the spin-orbit, split-off valence band to the conduction band is $E3$. The corresponding free exciton transitions are A, B, and C. According to Ref. 3 their transition frequencies at room temperature (293 K) are $\tilde{\nu}_{E1} = 14{,}112\ \mathrm{cm^{-1}}$ ($\lambda_{E1} = 708.6$ nm), $\tilde{\nu}_{E2} = 14{,}274\ \mathrm{cm^{-1}}$ ($\lambda_{E2} = 700.6$ nm), $\tilde{\nu}_{E3} = 17{,}538\ \mathrm{cm^{-1}}$ ($\lambda_{E3} = 570.2$ nm), $\tilde{\nu}_A = 13{,}983\ \mathrm{cm^{-1}}$ ($\lambda_A = 715.1$ nm), $\tilde{\nu}_B = 14{,}145\ \mathrm{cm^{-1}}$ ($\lambda_B = 707$ nm), and $\tilde{\nu}_C = 17{,}409\ \mathrm{cm^{-1}}$ ($\lambda_C = 574.4$ nm). The exciton binding energies are $E_{ex}(A) = E_{ex}(B) = E_{ex}(C) = 16$ meV ($= 129\ \mathrm{cm^{-1}}$). Bound exciton transitions occur at slightly longer wavelengths.[2,38] Even at room temperature, exciton transitions were identified in reflection measurements.[3] All the transitions are allowed for ordinary and extraordinary polarized light except the transitions $E1$ and A, which are allowed for only ordinary polarized light.[21,39,40] The binding energy of Se donors is 0.14 eV ($\approx 1128\ \mathrm{cm^{-1}}$).[2]

In Fig. 4 the refractive-index maxima coincide reasonably well with the band-edge transition wavelengths λ_{E1}, λ_{E2}, and λ_{E3}. Above the band edges anomalous dispersion occurs (Chap. 4 of Ref. 36). The increase in the refractive indices for $\lambda < 460$ nm is due mainly to a transition from the highest valence bands at the Γ point to the next higher conduction band and from the heavy-hole and spin-orbit, split-off valence band at the A point to the lowest conduction band. (Energy gaps are ~4 eV, see Fig. 1 on p. 442 in Ref. 2.)

In Fig. 5 the extinction coefficients κ and in Fig. 6 the absorption coefficients begin ~400 $\mathrm{cm^{-1}}$ below the band edges to rise roughly exponentially as expected from Urbach's rule.[41,42] The absorption below the band gaps $E1$, $E2$, $E3$ is though to be due to free-exciton (A, B, C),[3] impurity-bound-exciton (I_1, I_2, I_3),[2] and defect-bound-exciton transitions,[3,18] to transitions involving impurity states, and to phonon-assisted exciton transitions.[18,35,43] Detailed absorption measurements at the band edge are given in Refs. 12, 15, 16, 18, and 19. The absorption curves of Ref. 18 are included in Fig. 5. The exponentially rising absorption is shifted by ~10 nm to longer wavelengths compared with our crystal results, which indicated a higher concentration of impurities or crystal defects in the crystal of Ref. 18.

Neglecting impurity absorption and excitonic transitions, we expect the following frequency and wavelength dependences of the absorption and extinction coefficients for direct-gap semiconductors with parabolic bands[25,36,42]:

$$\alpha = \sum_i \beta_i (h\nu - h\nu_{E,i})^{1/2} \theta(\nu - \nu_{E,i})$$
$$= \sum_i \beta_i' (\lambda^{-1} - \lambda_{E,i}^{-1})^{1/2} \theta(\lambda_{E,i} - \lambda), \qquad (15)$$

$$\kappa = \frac{1}{4\pi c_0 \nu} \sum_i \beta_i (h\nu - h\nu_{E,i})^{1/2} \theta(\nu - \nu_{E,i})$$
$$= \frac{\lambda}{4\pi} \sum_i \beta_i' (\lambda^{-1} - \lambda_{E,i}^{-1})^{1/2} \theta(\lambda_{E,i} - \lambda), \qquad (16)$$

where i runs over the band transitions with $\lambda_{E,i} > \lambda$, β_i and $\beta_i' = \beta_i h c_0$ are characteristic constants, and $\theta(x)$ is the step function [$\theta(x) = 0$ for $x < 0$ and $\theta(x) = 1$ for $x \geq 0$]. In Fig. 6 the dashed curves are calculated by fitting Eq. (15) to the experimental curves at 600 and 500 nm. The short dashed curves show the contributions of the $E1$ and $E2$ transitions, and the dash–dotted curves show the contribution of the $E3$ transition. The enlarged experimental absorption coefficients below 500 nm are thought to be a result of deviations of the involved bands from a parabolic shape (the change in the density of states).

6. Conclusions

The principal optical constants n_o, κ_o, n_e, and κ_e of the uniaxial crystal CdSe have been determined in the strongly absorbing region above the valence band–conduction band energy gap by measuring the minimum reflectivity of parallel polarized light at the generalized Brewster angle. In the transparent sub-band gap region optical constants have been derived from normal-incidence transmission and Brewster-angle measurements. The applied special crystal orientations with the c axis perpendicular to the plane of light incidence (ordinary optical constants) and the c axis in the plane of incidence (extraordinary optical constants) permitted a separation of the principal optical constants from the measurements.

The described method may be applied to the determination of the principal optical constants of any optical uniaxial crystal.

References

1. D'Ans Lax, "Makroskopische Physikalisch-Chemische Eigenschaften," in *Taschenbuch für Chemiker und Physiker*, E. Lax, ed. (Springer-Verlag, Berlin, 1967), Vol. 1, p. 1-270.
2. I. Broser, R. Broser, and A. Hoffmann, "Cadmium selenide (CdSe)," in *Landolt–Börnstein Tables, New Series, Group III: Crystals and Solid State Physics, Vol. 17: Semiconductors: Subvolume b: Physics of II–VI and I–VII Compounds, Semimagnetic Semiconductors*, O. Madelang, ed. (Springer-Verlag, Berlin, 1982), pp. 202–224, 409–410, 442–457.
3. V. V. Sobolev, V. I. Donetskina, and E. F. Zagainov, "Direct precision method for detection of excitons in II–VI and III–V crystals at room and liquid nitrogen temperatures," Sov. Phys. Semicond. **12,** 646–652 (1978).
4. W. L. Bond, "Measurement of the refractive indices of several crystals," J. Appl. Phys. **36,** 1674–1677 (1965).
5. M. P. Lisitsa, L. F. Gudymenko, V. N. Malinko, and S. F. Terekhova, "Dispersion of the refractive indices and birefringence of CdS_xSe_{1-x} single crystals," Phys. Status Solidi **31,** 389–399 (1969).
6. R. L. Herbst and R. L. Byer, "Efficient parametric mixing in CdSe," Appl. Phys. Lett. **19,** 527–530 (1971).
7. S. A. Geidur and A. D. Yas'kov, "Dispersion of refractive index and photoelastic effect in semiconductors with a wurtzite structure," Opt. Spectrosc. (USSR) **48,** 618–622 (1980).
8. A. N. Pikhtin and A. D. Yaskov, "Refractive index and birefringence of semiconductors with the wurtzite structure," Sov. Phys. Semicond. **15,** 8–12 (1981).
9. B. Jensen and A. Torabi, "Refractive index of hexagonal II–VI compounds CdSe, CdS, and $CdSe_xS_{1-x}$," J. Opt. Soc. Am. B **3,** 857–863 (1986).
10. G. C. Bhar, "Refractive index interpolation in phase-matching," Appl. Opt. **15,** 305–307 (1976).
11. E. F. Gross and V. V. Sobolev, "Fine structure of the fundamental absorption edge in single crystals of cadmium selenide," Sov. Phys. Solid State **2,** 379–385 (1960).
12. R. B. Parsons, W. Wardzynski, and A. P. Yoffe, "The optical properties of single crystals of cadmium selenide," Proc. R. Soc. London Ser. A **262,** 120–131 (1961).
13. W. Wardzynski, "A method of measurement of a small birefringence," Acta. Phys. Pol. A **39,** 21–27 (1971).
14. I. V. Baranets, A. Kh. Zilbershtein, and L. E. Solovev, "Birefringence in crystals with isotropic points and determination of oscillator strengths for excitons in CdS by the Rozhdestvenskii hook method," Opt. Spectrosc. (USSR) **37,** 164–165 (1974).
15. S. P. Keller and G. D. Pettit, "Some optical properties of CdSe single crystals," Phys. Rev. **120,** 1974–1977 (1960).
16. W. Wardzynski, "Dichroism and birefringence of single crystals of cadmium selenide," Proc. R. Soc. London **260,** 370–377 (1961).
17. D. E. McCarthy, "The reflection and transmission of infrared materials: III, spectra from 2 μ to 50 μ," Appl. Opt. **4,** 317–320 (1965).
18. Č. Koňák, J. Dillinger, and J. Prosser, "The structure of the optical absorption edge in CdSe and CdTe," in *Proceedings of the Seventh International Conference on II–VI Semiconducting Compounds*, D. G. Thomas, ed. (Benjamin, New York, 1967), pp. 850–862.
19. N. R. Kulish, A. F. Maznichenko, and B. M. Bulakh, "Influence of laser radiation intensity on the edge absorption spectrum of CdSe," Sov. Phys. Semicond. **14,** 409–411 (1980).
20. M. Cardona and G. Harbeke, "Optical properties and band structure of wurtzite-type crystals and rutile," Phys. Rev. **137,** A1467–A1476 (1965).
21. J. O. Dimmock and R. G. Wheeler, "Exciton structure and Zeeman effects in cadmium selenide," J. Appl. Phys. **32,** Suppl. 10, 2271–2277 (1961).
22. M. Cardona, "Band parameters of semiconductors with zincblende, wurtzite, and germanium structure," J. Phys. Chem. Solids **24,** 1543–1555 (1963).
23. V. Dolocan, "Electrical, photoelectrical, and optical properties of CdSe thin films," Rev. Roum. Phys. **28,** 647–654 (1983).
24. R. C. Kainthla, D. K. Pandya, and K. L. Chopra, "Photoelectronic properties of solution-grown CdSe films," Solid-State Electron. **25,** 73–76 (1982).
25. A. A. El-Shazly, L. M. El-Nady, M. M. El-Nahars, H. T. El-Shair, and A. Y. Morsy, "Absorption of light in polycrystalline CdSe thin films in the region of the fundamental absorption edge," Opt. Pura Apl. **19,** 23–26 (1986).
26. Y. Lu and A. Penzkofer, "Optical constants measurements of strongly absorbing media," Appl. Opt. **25,** 221–225 (1986).
27. A. Penzkofer, M. Schäffner, and X. Bao, "Two-photon absorption and resonant non-phase-matched second-harmonic generation in CdSe," Opt. Quantum. Electron. **22,** 351–367 (1990).
28. W. König, "Elektromagnetische Lichttheorie," in *Handbuch der Physik, Vol. 20, Licht als Wellenbewegung*, H. Geiger and K. Scheel, eds. (Springer-Verlag, Berlin, 1928), pp. 141–262.
29. H. J. Eichler, "Dispersion und Absorption des Lichtes," in *Bergmann–Schaefer, Lehrbuch der Experimentalphysik, Band III: Optik*, H. Gobrecht, ed. (Walter de Gruyter, Berlin, 1987), pp. 207–324.
30. R. W. Ditchburn, *Light* (Academic, London, 1976), Chap. 15.
31. M. Born and E. Wolf, *Principles of Optics* (Pergamon, Oxford, 1980), Chap. 13.
32. M. V. Klein and T. E. Furtak, *Optics* (Wiley, New York, 1986), Chap. 2.
33. J. J. Hopfield and D. G. Thomas, "Theoretical and experimental effects of spatial dispersion on the optical properties of crystals," Phys. Rev. **132,** 563–572 (1963).
34. W. Leupacher and A. Penzkofer, "Refractive-index measurement of absorbing condensed media," Appl. Opt. **23,** 1554–1558 (1984).
35. D. H. Rank, "The index of refraction of air," in *Advances in Spectroscopy*, H. W. Thompson, ed. (Interscience, New York, 1959), Vol. 1, pp. 76–78.
36. D. L. Greenaway and G. Harbeke, *Optical Properties and Band Structure of Semiconductors* (Pergamon, Oxford, 1968).
37. B. Smandek, G. Chmiel, and H. Gerischer, "Photoluminescence as an *in-situ* technique to determine solid state and surface properties of semiconductors in an electrochemical

cell—application of the 'dead layer model'," Ber. Bunsenges. Phys. Chem. **93,** 1094–1103 (1989).
38. B. Segall and D. T. F. Marple, "Intrinsic exciton absorption," in *Physics and Chemistry of II–VI Compounds,* M. Aven and J. S. Prener, eds. (North-Holland, Amsterdam, 1967), Chap. 7, pp. 317–381.
39. D. C. Reynolds, C. W. Litton, and T. C. Collins, "Some optical properties of group II–VI semiconductors (I)," Phys. Status Solidi **9,** 645–684 (1965).
40. R. G. Wheeler and J. O. Dimmock, "Exciton structure and Zeeman effects in cadmium selenide," Phys. Rev. **125,** 1805–1815 (1962).
41. F. Urbach, "The long-wavelength edge of photographic sensitivity and of the electronic absorption of solids," Phys. Rev. **92,** 1324–0000 (1953).
42. J. I. Pankove, *Optical Processes in Semiconductors* (Dover, New York, 1971), Chap. 3.
43. R. E. Dietz, J. J. Hopfield, and D. G. Thomas, "Excitons and the absorption edge of ZnO," J. Appl. Phys. **32,** 2282–2286 (1961).